SANDIA REPORT

SAND2016-9569
Unlimited Release
Printed September 2016

The anatomy of the minority carrier - atomic cluster interaction in semiconductors

B. L. Doyle, E. C. Auden, E. Bielejec, J. B. S. Abraham and G. Vizkelethy

Prepared by
Sandia National Laboratories
Albuquerque, New Mexico 87185 and Livermore, California 94550

Sandia National Laboratories is a multi-mission laboratory managed and operated by Sandia Corporation, a wholly owned subsidiary of Lockheed Martin Corporation, for the U.S. Department of Energy's National Nuclear Security Administration under contract DE-AC04-94AL85000.

Issued by Sandia National Laboratories, operated for the United States Department of Energy by Sandia Corporation.

Available to DOE and DOE contractors from
U.S. Department of Energy
Office of Scientific and Technical Information
P.O. Box 62
Oak Ridge, TN 37831

Telephone: (865) 576-8401
Facsimile: (865) 576-5728
E-Mail: reports@osti.gov
Online ordering: http://www.osti.gov/scitech

Available to the public from
U.S. Department of Commerce
National Technical Information Service
5301 Shawnee Rd
Alexandria, VA 22312

Telephone: (800) 553-6847
Facsimile: (703) 605-6900
E-Mail: orders@ntis.gov
Online order: http://www.ntis.gov/search

SAND2016-9569
Unlimited Release
Printed September 2016

The anatomy of the minority carrier - atomic cluster interaction in semiconductors

B. L. Doyle, E. C. Auden, E. Bielejec, J. B. S. Abraham and G. Vizkelethy
Radiation-Solid Interactions Department 01111
Sandia National Laboratories
P.O. Box 5800
Albuquerque, New Mexico 87185-MS1056

Abstract

This project was to use light ion beam induced charge (IBIC) to detect damage cascades generated by a single heavy ion, and thereby reveal details of the shape of the cascade and the physics of recombination of carriers that interact with the cluster. Further IBIC measurements using the hardware and software of this project will improve the accuracy of theoretical models used to predict electrical degradation in devices exposed to radiation environments. In addition, future use of light ion IBIC detection of single ion-induced damage could be used to locate single ion implantation sites in quantum computing applications. This project used Sandia's Pelletron and nanoImplanter (nI) to produce heavy ion-induced collision cascades in p-n diodes, simulating cascades made by primary knock-on atoms recoiled by neutrons. Si and Li beams from the nI were used to perform highly focused scans generating IBIC signal maps where regions of lower charge collection efficiency were observed without incurring further damage. The very first use of ion channeled beams for IBIC was explored to maximize ionization, improve contrast and provide very straight line trajectories to improve lateral resolution.

ACKNOWLEDGMENTS

The expert technical skills of Stuart Van Deusen (01111) for developing two Amptek-based systems for performing deterministic ion implants on the Pelletron and ion-channeled IBIC on the Pelletron and nI is greatfully acknowledged, as is the proficiency of Daniel Perry in the operation and focusing of the nanoImplanter. In addition, the talents of Katherine Myers (17181) to mount the Amptek diodes and JFETs on the thermoelectrically cooled headers was greatly appreciated.

We also acknowledge the important interactions the PI (Doyle) had with Alan Huber, Bob Redus and John Pantazis of the Amptek company. They provided the first set of x-ray detector diodes for free, and gave us proprietary circuit designs of their XR100CR preamplifiers. Amptek was formed the same year the PI started at Sandia, 1977, and the electronics and detectors this company has developed over the years has had great utility in the Ion Beam Laboratory (IBL).

And finally we acknowledge John Bruce of the Scottish company SEMEFAB who provided the confidential details of the AXRCR-F x-ray detector diodes they make for Amptek. A nondisclosure agreement now exists between Sandia and SEMEFAB.

CONTENTS

FIGURES

TABLES

1. INTRODUCTION

Nuclear weapon electronics must continue operating following exposure to hostile gamma-ray and neutron radiation produced by the detonation of proximate nuclear weapons. The neutrons have very high energies, and when they collide with the nuclei of atoms in semiconductors, these atoms recoil at energies high enough to initiate collision cascades that form into clusters of atomic defects. These clusters are known to reduce electrical performance (e.g. transistor gain) by promoting electron-hole recombination and capturing carriers flowing in semiconductor devices. Unfortunately a detailed understanding of the carrier-cluster physics has remained elusive and the effects have only been qualitatively understood and modeled. This LDRD was to fill this gap of understanding by performing an experiment that examines the physics of electron-hole recombination in and around these clusters on a nanometer scale. The experiment was to quantify the flow and attenuation of carrier density around a single nm-sized cluster, and the results were to be understood by modeling the carrier drift, diffusion and recombination physics.

The importance of the carrier-cluster interaction on gain degradation was revealed by the Qualification Alternatives to the Sandia Pulsed Reactor, or QASPR, program [1]. The reduction of transistor gain following broad ion beam and neutron exposures have been successfully compared to the QASPR-developed Wampler-Myers model [2,3] of electron-hole recombination currents near these clusters, but this has provided only a macroscopic phenomenological understanding. This LDRD can be thought of as a spin-off of this part of the QASPR program, and the plan was to have QASPR complete some of the measurements that can validate aspects of the model. The idea of this project was that when the focused ion beam crossed through a cluster, or simply grazed one, that enhanced electron-hole (e-h) recombination would reduce the charge induced and collected in the IBIC experiment, thereby revealing the shape and size of the cluster. Detailed measurements of the reduction of the IBIC signal would then be compared with the Wampler-Myers theory.

Experiments first utilized the Pelletron-μBEAM in the Ion Beam Laboratory (IBL) to perform the microbeam scanned Ion Beam Induced Charge (IBIC). Section 2 below describes these first IBIC experiments on the Peletron-μbeam which were used to 1) identify the best diode devices to be used, 2) to reduce the noise in the diode-preamplifier-amplifier IBIC measurement system, 3) to perfect performing IBIC with channeled ions (i.e. aligned with major crystallographic axes), 4) to perfect single implanted ion detection for the deterministic (i.e. counted) heavy ion implants. Descriptions of the two IBIC systems developed for the nI are also given in this Materials and Methods Section.

In Section 3 we outline the IBIC experiments performed on the unique nanoImplanter (nI) in the IBL to observe the enhanced e-h recombination in lateral oriented diodes implanted with both low to high fluences of heavy ions. Here the nI was used to both 1) produce the high fluence implants resulting in clusters and collision cascades and 2) to inject the carriers and measure the collection efficiency of these carriers using IBIC. The nI was also used in an early attempt to map individual cascades made by implanting high energy Xe ions into a lateral pn diode. The IBL is the only lab in the US that could perform this first-of-it's-kind experiment.

The planning of performing nanobeam IBIC on single defect collision cascades and clusters is discussed in Section 4. Most of these results came during the last year of the LDRD project. This included the discovery that by channeling the ions from both the Pelletron and nI, that the IBIC signal increases markedly, and the resolution of this signal was greatly improved. These benefits were the result of almost completely removing the scattering that occurs between the ion and atoms in the diodes. The effect of this scattering is stochastic, and not only reduces the IBIC signal, that only depends on ionization, but also degrades the IBIC resolution. This effect is known as nuclear deficit [4].

A conclusion and recommendation for future work to be funded by the QASPR program is found in Section 5.

2. MATERIALS AND METHODS

The first part of this project involved testing numerous preamp and diode combinations to find those with the lowest IBIC signal noise. This was very important because the decrease in charge induction when a single ion passes through regions of a collision cascade or cluster was expected to be very low. Maximum contrast of the IBIC signal was therefore critical. Because of its availability, most of these experiments utilized the Pelletron-μBEAM instead of the IBL nI. This μBEAM could focus 3 MeV protons or 0.75 MeV alpha particles for the IBIC experiments to sub micron dimensions, but this resolution was not adequate to reveal the details of single collision cascades which extend only 100s of nm. Nevertheless, the Pelletron-μBEAM proved to be an ideal platform with which to perfect not only the ultra high resolution IBIC signal, but also the deterministic (i.e. individually counting the number of implanted ions) heavy ion implants that produced the collision cascades. The details of this optimization can be found in reference [5], and we only summarize those results here.

2.1. Optimizing IBIC signal resolution

In reference [5] we showed how optimal detector / pre-amplifier combinations were identified for the use of light ion IBIC (ion beam induced charge) to probe the physical structure of electrically active defects in damage cascades caused by heavy ion implantation. The ideal detector needed to have a sufficiently thin dead layer so that incident ions produced the majority of damage cascades in the depletion region of the detector rather than the dead layer. Detector and circuit noise must be low enough to detect the implantation of a single heavy ion as well as the decrease in the light ion IBIC signal caused by Shockley-Read-Hall recombination when the beam scans regions of the detector damaged by the heavy ion. The IBIC signals from three detectors irradiated with 750 keV He+ ions were measured with commercial charge sensitive pre-amplifiers to identify the combination with the lowest noise.

2.1.1. Diodes and Circuits

2.1.1.1. DPAD/APD diodes and A250 circuit

The circuit that initially provided the best resolved IBIC signal is shown in Figure 1, and a scanned IBIC median filtered image of a Linear Systems DPAD is given in Figure 2. The DPAD diodes [6] had their ~1μm SiO_2 and Si_3N_4 passivation layers removed by etching, and best results were obtained with the Amptek A250 pre-amp circuit [7] mounted inside the vacuum chamber where the microbeam IBIC was performed. The DPAD diode was also mounted within this A250 circuit to minimize the distance to the FET of this pre-amp. The best IBIC signal resolution obtained with the DPAD/A250 preamp combination was 1.24 keV using the 750 keV He+ ions from the Pelletron.

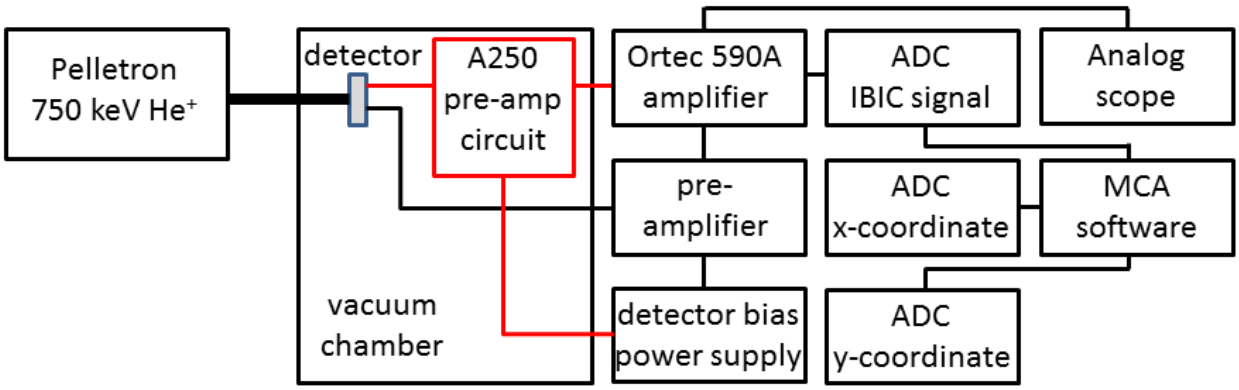

Figure 1: Diagram of experimental setup used to read IBIC signals from detectors irradiated with 750 keV He+ ions.

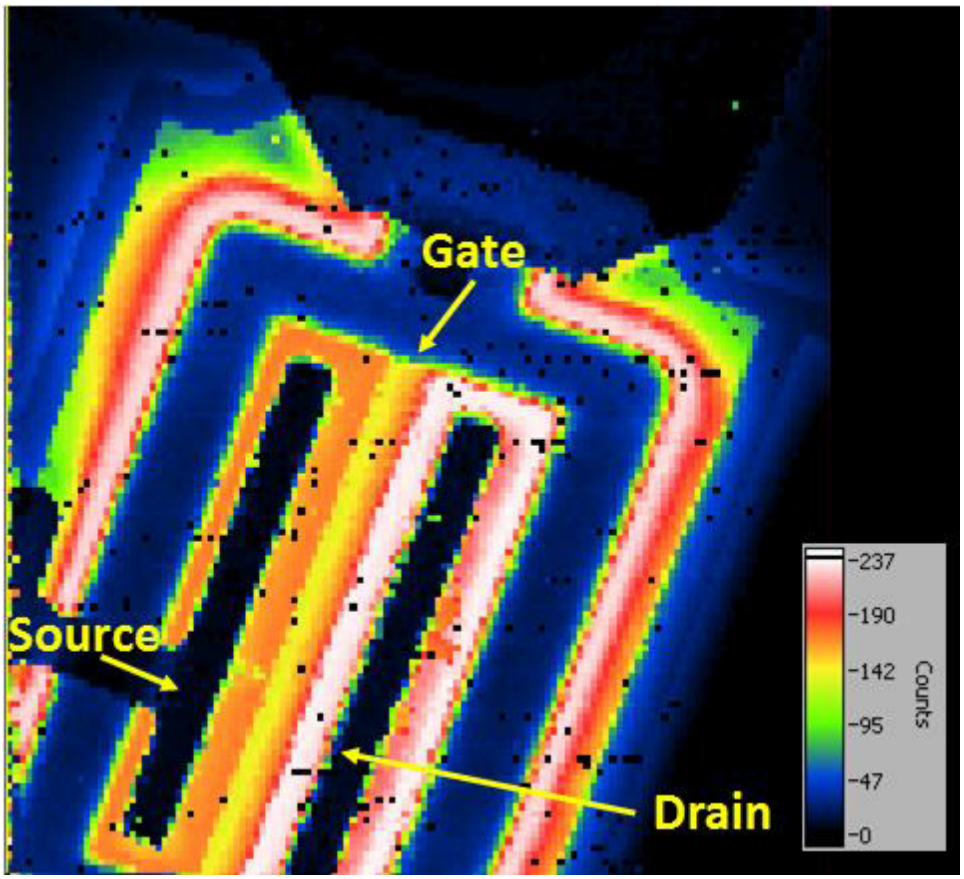

Figure 2: IBIC signal from an etched DPAD5 detector irradiated with 750 keV He+ ions

One of the diode/pre-amplifier combinations that we originally thought would provide the best resolution was the DPAD/Amptek CoolFET system [8]. This high resolution was anticipated because the temperature of the FET in the CoolFET was reduced to ~200K with a thermoelectric

cooler to reduce noise and improve energy resolution. Unfortunately it was then not possible to place the CoolFET in the vacuum system where the IBIC was performed, which also meant that we couldn't place the DPAD inside the CoolFET in close proximity to the cooled FET. This combination only produced an IBIC signal with a resolution of ~9 keV.

To summarize, the key advantage of the simple A250 pre-amplifier circuit was that it can be placed inside the vacuum chamber with the detector. The interconnect wires were on the scale of millimeters rather than meters, and this reduces the capacitance and thermal noise associated with cables and interconnects that were processed by the preamplifier along with the IBIC signal. The CoolFET cannot be operated inside the vacuum chamber without a heat sink for the Peltier cooler, and it was unknown whether the components inside the Ortec 142A can be cooled along with the detector or whether this pre-amplifier can operate in the vacuum chamber without a heat sink.

2.1.1.2. Amptek AXRCR-F diode and XR100CR/PX5 circuit

The potential improvement provided by both cooling the FET and minimizing the diode-FET distance led the project to consider using an Amptek AXRCR-F x-ray detector diode [10] for the IBIC experiment. The layout of this detector is shown in Figure 3. Note that both the FET (actually a JFET) and Si PIN s-ray detector diode are both cooled, and that they are mounted on the thermoelectric cooler very close together.

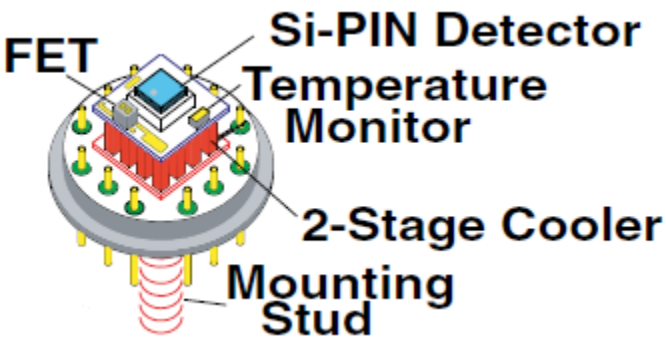

Figure 3: Layout of Amptek AXRCR-F x-ray detector.

Because these detectors are expensive, unmounted diodes and JFETs, manufactured by the SEMEFAB Company [11] were acquired from Amptek. A nondisclosure agreement (NDA) was executed between SEMEFAB and Sandia, and they provided the design details of the detector diodes. Katherine Myers (17181) of the MDL packaging group became adept at mounting both the Si PiN diode detectors and JFETs onto the thermoelectrically cooled headers.

The circuit used to process the IBIC signals produced when ions from both the Pelletron and nI struck the AXRCR-F PIN diodes is shown in Figure. 4.

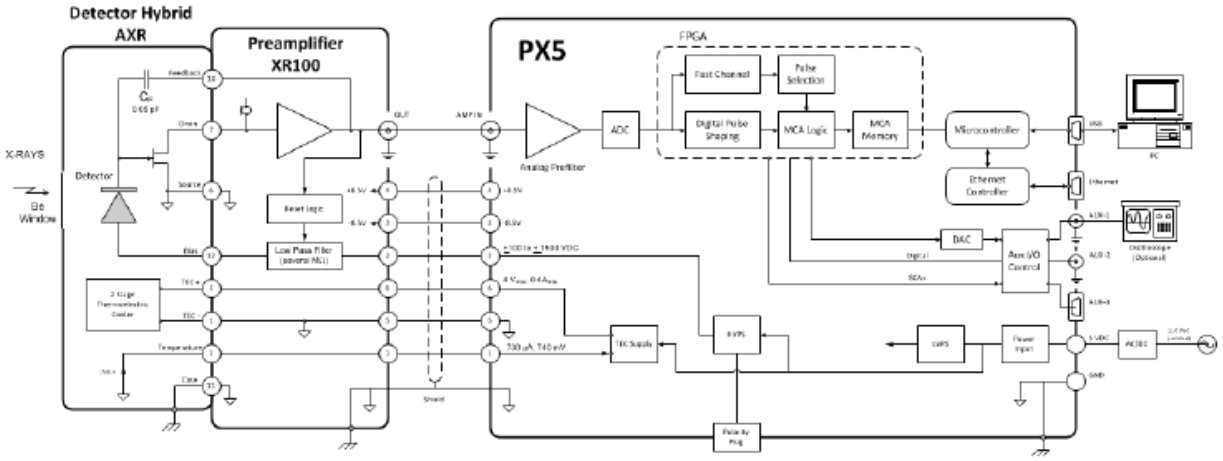

Figure 4: Block diagram of the PX5 connected to an Amptek XR100 detector.

The circuits acquired from Amptek represented a nuclear spectroscopy system including (1) the detector (which in our case was the Si crystal sample in which to implant heavy ions producing damage clusters, followed by microbeam and nanobeam IBIC), (2) the XR100 preamplifier, (3) the PX5 pulse processing electronics (which include pulse shaping, pulse selection logic, pulse counters, a multichannel analyzer, and interfaces for data acquisition and control), (4) the power supplies, and (5) the computer running software for instrument control, data acquisition, and data analysis. The PX5 is a single board digital pulse processor which implements the functions described in (3) above. A typical spectrum of Mn K-alpha and K-beta xrays (~6 keV) from a ^{55}Fe source is shown in Figure 5. The resolution of the system was measured to be ~150 eV, even for those diodes and JFETs mounted by the MDL.

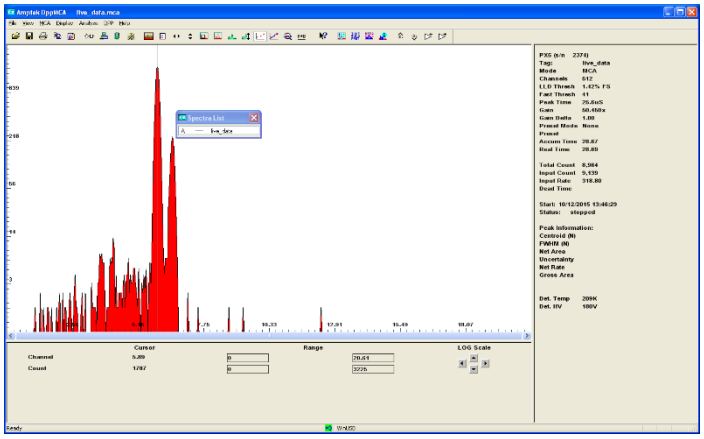

Figure 5: X-ray spectrum from ^{55}Fe source showing 145 eV resolution.

In Figure 6 we plot a summary of the IBIC resolution obtained by the different DPAD-Pre-amp and Amptek AXRCR-F diode/XR100CR pre-amp combinations.

Figure 6: The progression of IBIC energy resolution for DPAD and Amptek diodes.

Two of the Amptek systems were developed. The first was used for the deterministic heavy ion implants made by the Pelletron to produce collision cascades and clusters of defects in the Si crystal diodes. The second was used in the nI for the ion-channeled IBIC experiments and is described in detail below.

2.1.2. Channeled-Ion IBIC

This first system was also used to explore the use of microbeam channeled-ion IBIC to improve the energy resolution of the technique. The idea here was that by orienting the crystal diodes for channeling of the ions, that the IBIC signal would increases markedly, and the resolution of this signal would be greatly improved. These benefits would be the result of almost completely removing the scattering that occurs between the ion and atoms in the diodes. The effect of this scattering is stochastic, and not only reduces the IBIC signal, that only depends on ionization, but also degrades the IBIC resolution.

The Amptek AXRCR-F detector header was mounted onto a high resolution 3-axis channeling goniometer system developed for materials analysis. A flexible cable attached the header to the XR100CR pre-amp that was also in the vacuum system, and a signal cable took the output of the pre-amp to the PX-5 digital amplifier, which was mount outside the vacuum system.

300 keV alpha particles and Kr+ ions were accelerated by the Pelletron and collimated in the channeling beam line before impinging on the Si crystal diode that was reverse biased. The IBIC signal distribution for the case where the Si crystal was oriented for <001> axial channeling and randomly oriented for the alpha particles is shown in Figure 7, and for the Kr+ ions in Figure 8.

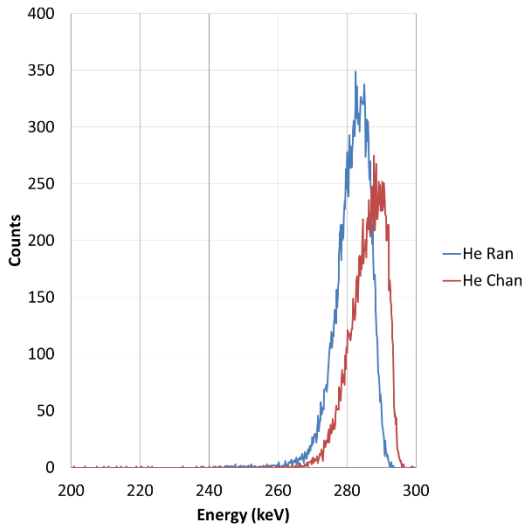

Figure 7: 300 keV alpha IBIC signal pulse height distribution for channeled and randomly oriented Si crystal diode. The x-axis has been converted to ion energy.

From the alpha particle data in Figure 7, it is clear that the IBIC signal pulse height increases as expected. The resolution improvement can also be seen by examining the sharpness of the front edge. This data confirmed that the beam to eventually be used on the nI should be channeled. A 2-axis goniometer would therefore be needed to hold and orient the Si diode crystal for the experiments to observe the e-h recombination induced reduction of the IBIC signal.

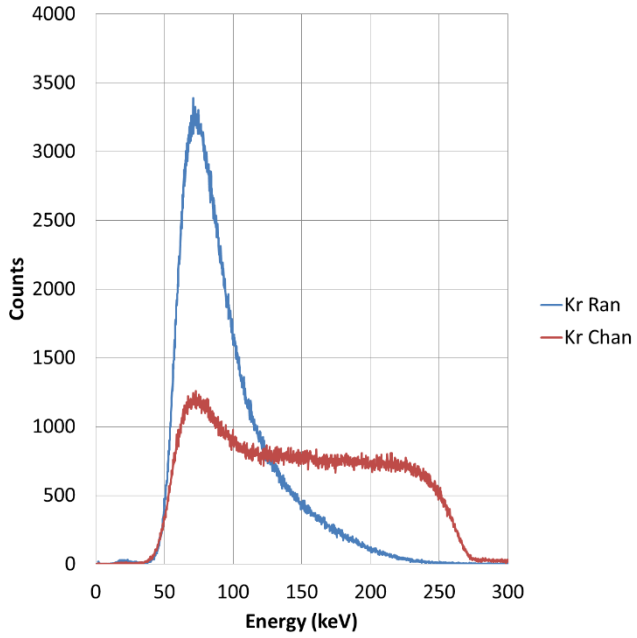

Figure 8: 300 keV Kr+ IBIC signal pulse height distribution for channeled and randomly oriented Si crystal diode. The x-axis has been converted to ion energy.

For the Kr+ IBIC shown in Figure 8, the energy distributions for the two orientations, channeled and random, indicate several things:

1. The front edge of the channeled Kr is at ~260 keV indicating that there remains a thin 10-20 nm native oxide on the surface.
2. The wide fairly flat energy distribution of the channeled IBIC demonstrates that dechanneling is occurring resulting in lower ionization.
3. For the random case, the high energy tail suggest some ions scatter into channels where ionization is greater.
4. For the channeled case, Marlowe calculations significantly overestimated the contribution to ionization caused by the primary ion knock-on recoils.

2.2 Ion Implantation induced collision cascades and defect clusters

2.2.1. Low Fluence Deterministic Implants on the Pelletron

The IBIC signal shown in Figure 8 for the random case and the Pelletron-accelerated 300 keV Kr beam (and 1.6 MeV Xe – not shown) was used for the deterministic implants. Two fluences were used 10^6 and 10^7 ions/cm^2 resulting in collision cascades being made either 10 μm or 3 μm apart, on average, respectively. These implant fluences are summarized in Table 1.

			average
	Energy	Fluence	separation
Beam	(MeV)	#/cm2	um
Xe+	1.7	1.00E+07	3.16
Kr+	0.3	1.00E+06	10
Kr+	0.9	1.00E+07	10

Table 1: Low fluence beams implanted into Amptek AXRCR-F diodes

2.2.2. High Fluence Implants on the nanoImplanter

200 keV Si++ beams from the IBL nI were also used to produce 0.5x0.5 μm square patches of defect clusters in Si detectors being developed as avalanche photo detectors (APDs) for another project. Details of these implants and the subsequent IBIC analysis using 100 keV Li+ ions can be found in Reference [12] and is only briefly covered here.

The nanoImplanter is a 100 keV machine that can accelerate doubly-charged ions to a maximum energy of 200 keV. The nanoImplanter includes an E×B filter capable of switching ion species and energies without changing the beam location with respect to the stage. The Si++ ions were supplied from an AuSiLi liquid metal alloy ion source (LMAIS). Areas of increased displacement damage were also generated with the nanoImplanter by rastering 200 keV Si++ ions across the localized 0.5x0.5 μm square regions. The maximum energy of the nanoImplanter of 200 keV was chosen for the Si beam to maximize both the amount of damage created by each Si ion and the depth under the device surface at which damage clusters would occur. Table 2 summarizes the Si implants performed on the nI and used in the high fluence part of this research.

ION DENSITIES AND DISPLACEMENT DAMAGE DOSE IN DAMAGED AREAS

Number of Ions	Damage Area (μm × μm)	Ion Density (ions/μm^2)	D_d (MeV/g)
20,000	0.5 × 0.5	80,000	6.24×10^{15}
10,000	0.5 × 0.5	40,000	3.12×10^{15}
5,000	0.5 × 0.5	20,000	1.56×10^{15}
1,000	0.5 × 0.5	4,000	3.12×10^{14}
Background	4.0 × 4.0	1,250	9.75×10^{13}
10,000	0.1 × 0.1	1,000,000	7.80×10^{16}
10,000	0.5 × 0.5	40,000	3.12×10^{15}
10,000	1.0 × 1.0	10,000	7.80×10^{14}
Background	4.0 × 4.0	1,250	9.75×10^{13}

Table 2: Ion densities and displacement damage dose in Si Implanted APDs.

2.3 Ion Beam Induced Charge (IBIC) measurement systems

There were two types of IBIC experiments made in this project. The first was to perfect the IBIC technique using the Si implanted patches on the APD samples made on the nI and 1.6 MeV Xe implants on the DPADS. The second was to look for individual collision cascade clusters made by the 300 keV Kr implants on the Pelletron, using focused and channeled 100 keV Li+ ions on the nI.

2.3.1. IBIC on the APD and DPADs

For the Si APDs damaged with the 200 keV Si++ beams from the nI, Si IBIC scans were performed after Si damage generation. 60 keV Li IBIC scans were also performed. The detector was biased at 0 V during IBIC measurements, so the width of the depletion region around this *pn*-junction depends only on the junction's built-in bias. In this work, IBIC scans were performed by rastering the ion beam over a quasi-neutral region of the APD. These APD samples were held at or near room temperature in a specially designed target holder cassette that was introduced through a load lock on the nI.

A CoolFET pre-amplifier was used to convert the current pulse caused by ion-induced e-/h pair generation into a voltage pulse [21]. To reduce noise and improve IBIC signal resolution, the pre-amplifier signal was first input to a SIM965 low-pass filter and then to two SR200 boxcar averagers. The first boxcar was triggered to sample the pre-amplifier response immediately before the beam blanker was released; this boxcar measures the pre-amplifier response just before the ion pulse strikes the detector. After a delay of 50 μs, the second boxcar samples the pre-amplifier signal at the height of its response to the ion pulse. The 50 μs delay accounts for the rise time of the CoolFET response to the ion pulse. The outputs of both boxcars were input to a SIM980 summing amplifier. The IBIC response was recorded in mV as the difference between the boxcar signals. The two-boxcar measurement technique filters low and high frequency noise from the pre-amplifier signal.

2.3.2. Channeled IBIC on the Amptek AXRCR-F x-ray detector diodes

For the Si x-ray detector diodes made by Amptek, and mounted by the MDL, a special cassette for the nI was made that held the AXRCR-F diode header on a two axis Attocube goniometer [13]. This header was then connected to a XR100CR pre-amp mounted in the cassette that gets inserted into the nI through a load lock. When inserted through this load lock, electrical connections were made that go outside the nI to the controls of the Attocube goniometers and connections between the pre-amp and the PX-5 digital amplifier. An analog IBIC signal from the PX-5 was then fed to a pulse height analysis (PHA) analog to digital converter (ADC) of a FastCom MPA-3 multiparameter data acquisition system [14]. A Labview program was written to send sawtooth DC low voltage waveforms to a high voltage operational amplifier that drives the HV scan plates of the nI. These low voltage waveforms were also sent to Sample Voltage Analysis (SVA) ADCs that recorded the x-y position of the beam during it's scan in coincidence with each IBIC pulse measured. This unique system is shown and labeled below in Figure 9.

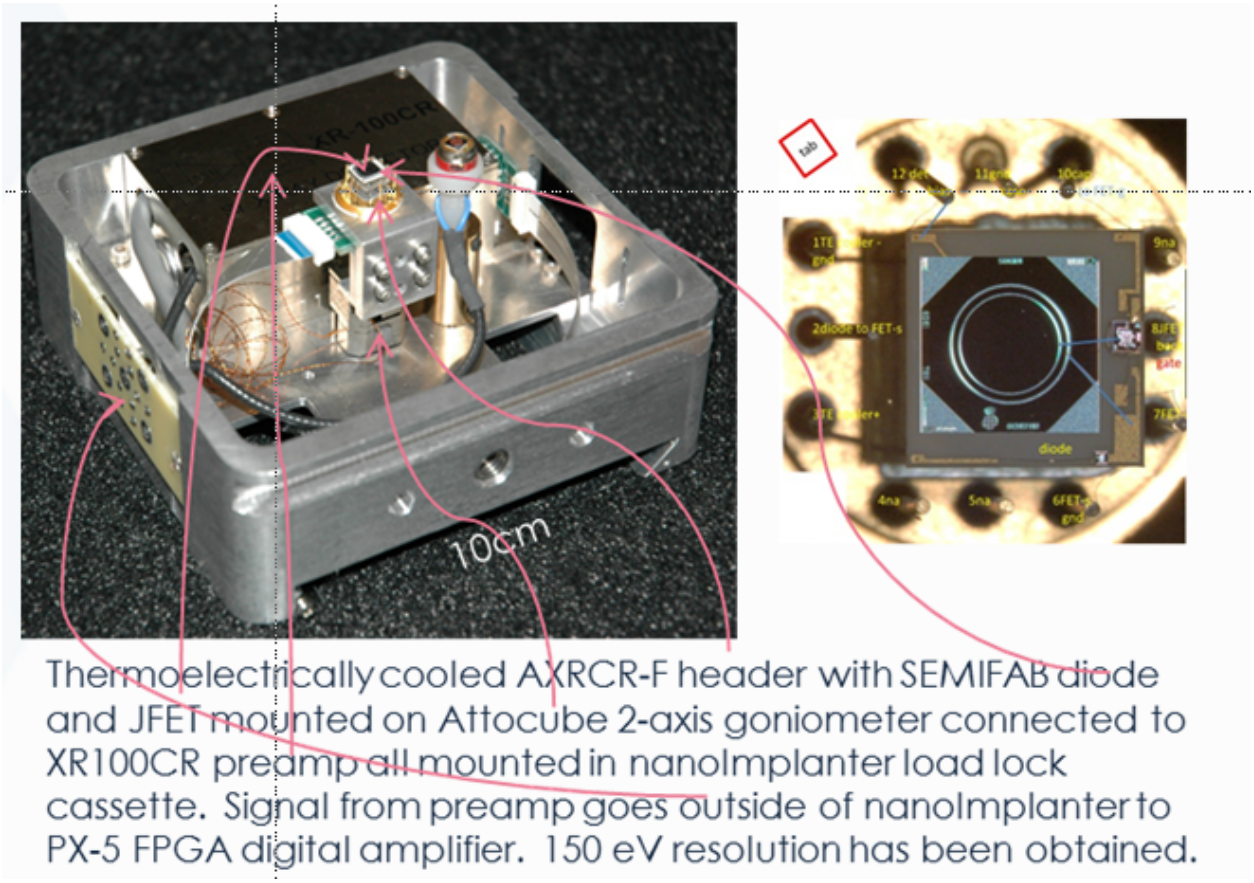

Figure 9: Load-lock Cassette for nI that has Amptek detector, preamp and goniometer.

3. INITIAL IBIC EXPERIMENTS ON NANOIMPLANTER

In this section, we outline the IBIC experiments performed on the nanoImplanter (nI) in the IBL to observe the enhanced e-h recombination in lateral oriented diodes implanted with both low and high fluences of heavy ions. Details of these implants can be found above in Section 2.2. These heavy ions in turn produce collision cascades and defect clusters in the regions implanted. The reduction of the IBIC signal in these regions were then measured using the equipment described above in Section 2.3.

3.1. High fluence implanted APD results

As mentioned above, the nanoImplanter was used at its maximum potential of 100kV to implant 200 keV Si++ into lateral diodes APDs. The nanoImplanter includes an E×B filter capable of switching ion species and energies without changing the beam location with respect to the stage. The Si++ and Li+ ions were supplied from an AuSiLi liquid metal alloy ion source (LMAIS), and selected using the ExB filter. The Si IBIC scans were performed ~10 minutes after Si damage generation. The Li beams proved more difficult to generate, and IBIC scans were performed ~7 months after the Si IBIC scans. Again, these results are explained in much more detail in our paper found in reference [12].

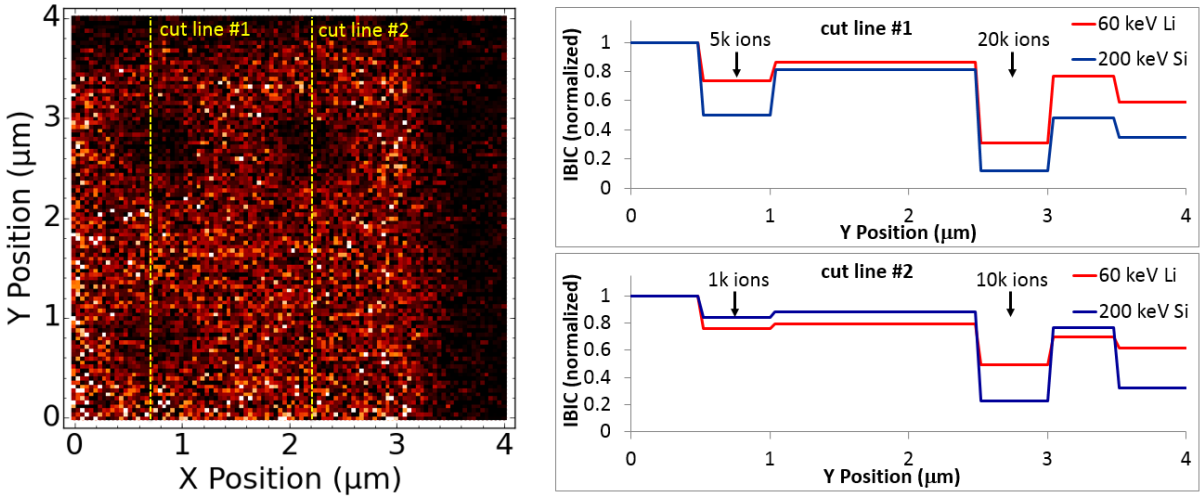

Figure 10: Normalized IBIC for two cutlines taken across the detector damaged with 200 keV Si ions. Cutlines are overlain on the IBIC map shown in Fig. 5b. The anode (not shown) is located at y = 9.5 µm. The cathode (also not shown) is located at y = -30.5 µm. The two plots on the right shown normalized Q/Q0 vs. y-position for 200 keV Si++ IBIC and 60 keV Li+ IBIC.

The average IBIC signals measured from Si and Li IBIC scans are shown in Fig. 10 as blue lines (Si) and red lines (Li). IBIC values have been normalized to the average value in the background region between y = 0 μm and y = 0.5 μm where Fig. 9 shows that the average IBIC signal is highest. At this position, holes may recombine in the two damaged regions between y = 0 μm and the anode, but electrons can drift to the cathode located ~30 μm away without suffering much recombination.

Fig. 10 shows that average IBIC values are reduced compared to background over regions damaged by 1,000, 5,000, 10,000, and 20,000 ions. The largest IBIC reduction was measured over the region damaged with 20,000 Si ions, and the least IBIC reduction for a damaged area corresponds to the region damaged with 1,000 Si ions. The background region between the two damaged regions from y = 1.0 μm to y = 2.5 μm exhibits lower IBIC values than the background region between y = 0 μm and y = 0.5 μm. Although this region was not purposefully damaged with Si ions, carriers generated within this region were subject to recombination as they diffuse into the nearby damaged regions, so the IBIC signal is reduced.

To conclude, localized regions of IBIC signal reduction were apparent in IBIC maps generated by rastering 200 keV Si++ ion across a Si detector that has been damaged with closely spaced pulses of 200 keV Si++ ions. IBIC signal reduction can be resolved for damage caused by as few as 1,000 ions of Si rastered over a 0.5 μm × 0.5 μm area. The area of IBIC signal reduction was larger than the area rastered with the damaging ions, indicating that the IBIC measurement was sensitive to e-/h pairs which were generated in undamaged regions but must drift through damaged regions. This is of critical importance to modeling the effects of the localized damage clusters on device operation. These results also gave confidence that the nI scans over individual clusters should show a measureable decrease in the IBIC signal. For example, the 1000 Si/.25μm^2 exposure reduced the IBIC signal by 20%, if the resolution of IBIC is brought down to 1% using the Amptek x-ray detectors and associated electronics (actually if this resolution remains 0.15 keV and the beam is 200 keV Si, then that is even better than 1%), then scaling the results above we should be able to see the effect on IBIC of 1 ion/0.005μm^2 which is ~70nm on a side. The nI can produce beams with a spotsize of ~20nm, therefore we should be able to have enough contrast in the IBIC signal to "see" the clusters.

3.2. Low fluence implanted DPAD results

The IBL Pelletron was used to expose etched DPAD diodes to low fluences of 1.4 MeV Xe ions optimized for spacing of one Xe ion per 3 μm^2 as described in Section 2.2.1. Damage clusters were not detected through EBIC performed with org. 1755 or with IBIC performed with 750 keV alpha particles in the IBL Pelletron μBEAM. Localized Xe damage detection performed in the IBL NanoImplanter with 17 scans of 160 keV Si was inconclusive (see Fig. 1), and the overall IBIC signal degraded with successive scans of the Si beam.

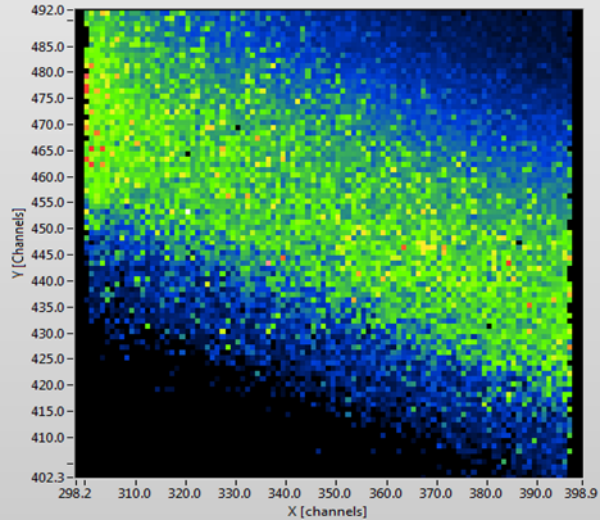

Figure 11: 160 keV scanned IBIC on DPAD implanted with 1.e8 1.4 MeV Xe/cm^2 . The region shown is ~5 μm on a side.

Defect cluster effects on EBIC and IBIC signals were modeled in 2D and 3D. Figure 12 shows the theoretical IBIC measured Charge Collection Efficiency (CCE) scanning a 100 keV Li ion in the vicinity of a 100nm diameter cluster.

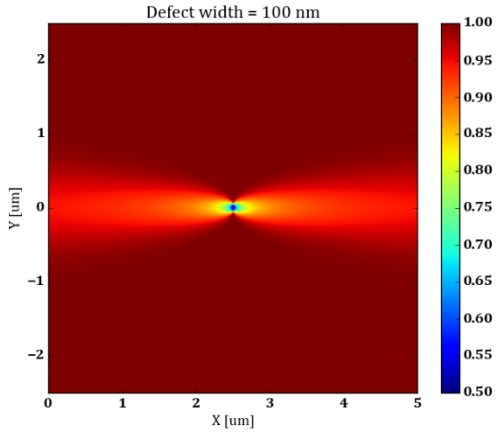

Figure 12: the theoretical IBIC measured Charge Collection Efficiency (CCE) scanning a 100 keV Li ion in the vicinity of a 100nm diameter cluster.

Channeled Li was determined to be the optimal light ion to detect single ion-induced defect clusters. While Si beams have been used to detect damage from ~5,000 heavy ions as shown above in Section 3.1, modeling and experiments during have determined that Si IBIC was insufficient to detect single clusters. The vacancies distributions made by the 1.4 MeV Xe, nonchanneled 0.16 MeV Si and 0.1 MeV Li were calculated using the Marlowe code [15] and are plotted in Figure 13.

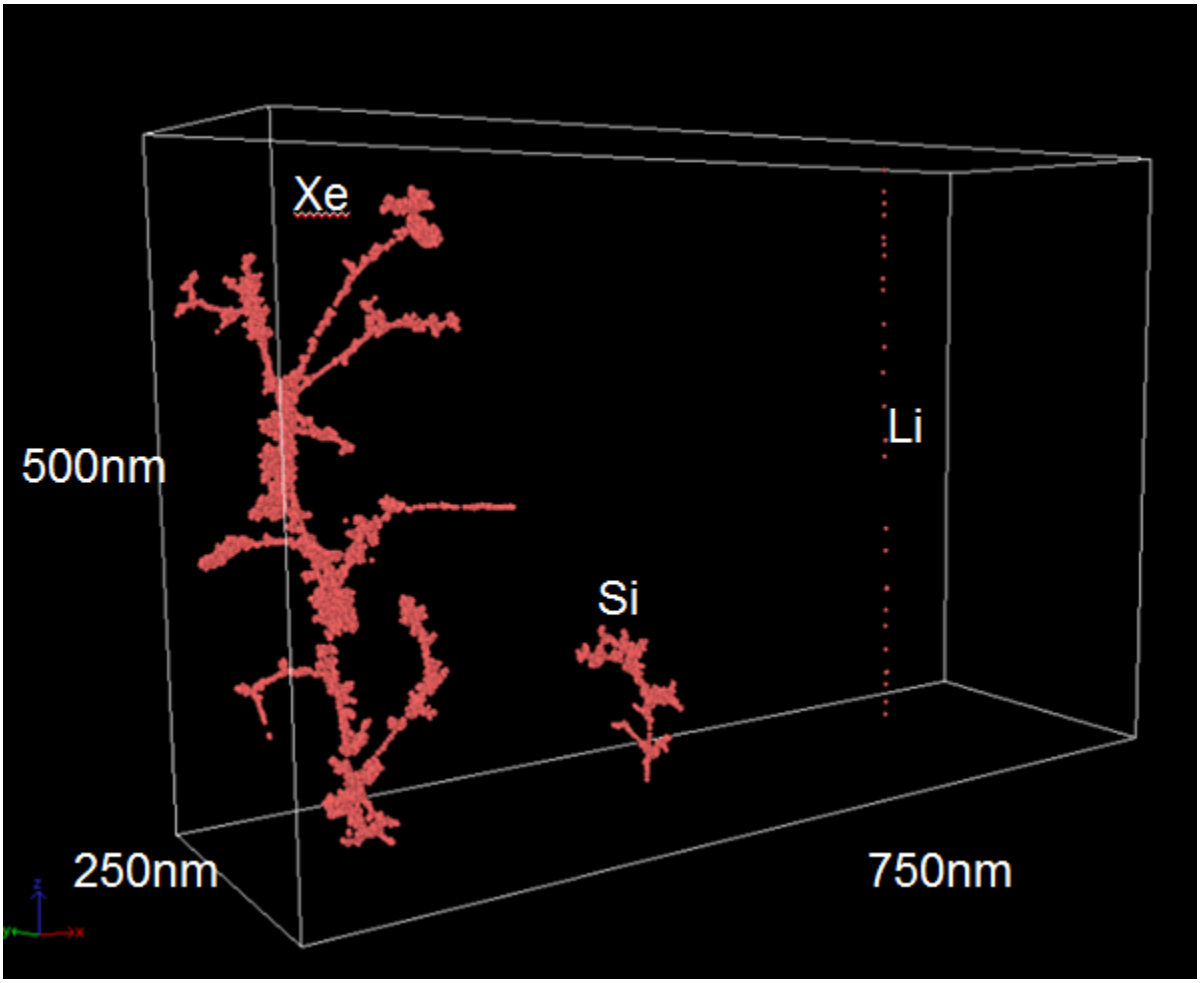

Figure 13: Lateral and depth distribution of 1.4 MeV Xe, nonchanneled 0.16 MeV Si and 0.1 MeV Li implanted (from the bottom of the figure) into Si.

In this figure it is clear that the Si beam that was used in the first attempt to observe the reduction in IBIC caused by the defect distribution made by implanting 1.4 MeV Xe into Si was not seen. This is because: 1) Si produces too much damage, 2)the nuclear deficit for Si is large, 3) range of Si is much less than the 1.4 MeV Xe, 4) the trajectory of nonchanneled Si spreads out laterally too much. All of these effects degrade the contrast of IBIC and makes resolving a single defect-cluster impossible with Si. But these effects were eventually mitigated by using a channeled Li beam for IBIC and are discussed in the next section.

4. FINAL IBIC EXPERIMENTS ON NANOIMPLANTER

The culmination of nearly 3-years of R&D was to occur in the last quarter of this LDRD. This was to involve mapping of 100 keV Li+-ion IBIC around single defect clusters made by collision cascades of 300 keV Kr implanted using the Pelletron into Si diodes.

4.1. Li+ beam on nanoImplanter

A Li+ beam was obtained from the nanoImplanter (nI) by using a SiAu(Li) liquid metal ion source. The beam current of the Li+ was measured in a Faraday Cup in the nI to be in the picoAmp range. The energy of the beam was limited by sparking of the HV power supply of the nI above 50 kV. The beam energy was therefore 50 keV for the Li+ ions. A plot of the mass scan on the nI using the SiAu(Li) source is shown in Figure 14.

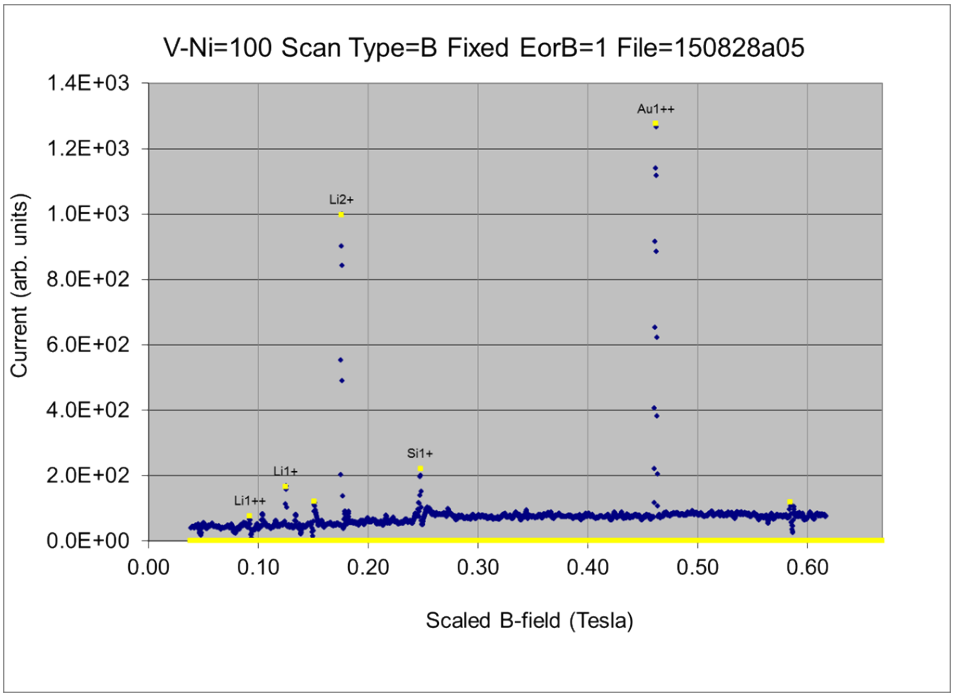

Figure 14: Magnetic field scan of the ExB filter of the nI. These were all the ions produced using the SiAu(Li) source. The Li+ current was of the order of a picoAmp.

The ExB filter was set for the Li+ beam was then focused onto a wire cross. A picoAmp beam, while small, was still far too intense for performing IBIC, and this current needed to be reduced by over a factor of 1000.

4.2 Reducing beam current to a few 100 ions

This reduction of beam current was accomplished by reducing the first condenser lens of the nI to ½ its normal value. This defocused the nI Li+ beam at the position of the first aperture, and reduced the current to a manageable level of several 100 to a few 1000 ions/sec. The resolution

of the beam was measured by scanning the beam across the bias electrode of the Amptek diode x-ray detector, and found to be <100nm. It was somewhat surprising that the beam retained a fairly good focus following the defocusing applied to the first lens, but ion optics calculations confirmed that while the Li+ beam had three cross-overs in the focused setting of this first lens, that when defocused, there were only two cross-overs, and the beam retained a fairly good focus. The results of the ion optic calculations are shown in Figure 15.

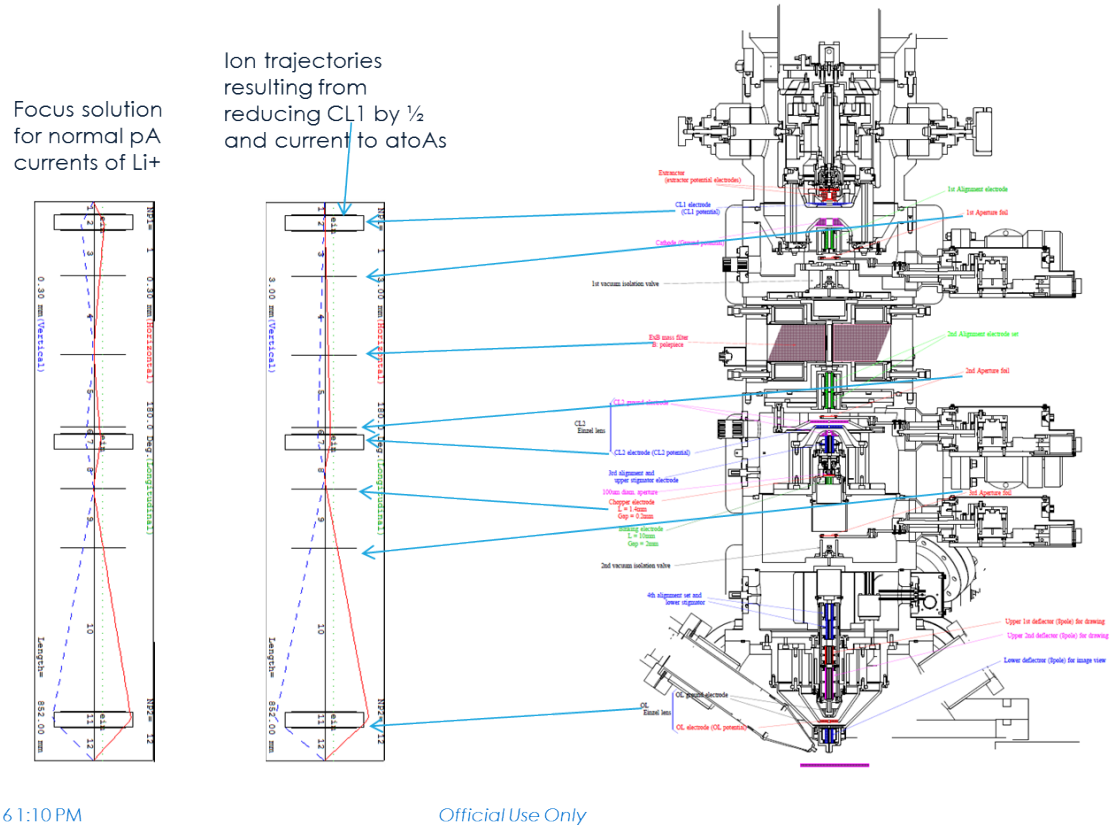

Figure 15: Ion optics calculations of the focus condition (far left) resulting in pA beams of Li+, and the defocused lens 1 condition that reduced the current to a few 100 ions/sec, but retained a good focus on target. A cross section of the nl is shown at the far right.

The thermoelectrically cooled Amptek x-ray detector and JFET plus the XR100CR preamplifier and PX5 amplifier described in Section 2.1.1.2 was used to perform the scanned IBIC validating this high resolution.

4.3 Channeling the Li+ ions in the Amptek diode crystal

Channeling contrast of 50 keV Li+ IBIC signals were observed by recording the IBIC signal while rocking the two axes of the Attocube goniometer. This goniometer's two rotation axes were orthoganal to each other and labled θ and φ. The median of the IBIC pulse height signal as a function of the tilt angle θ is plotted in Figure 16.

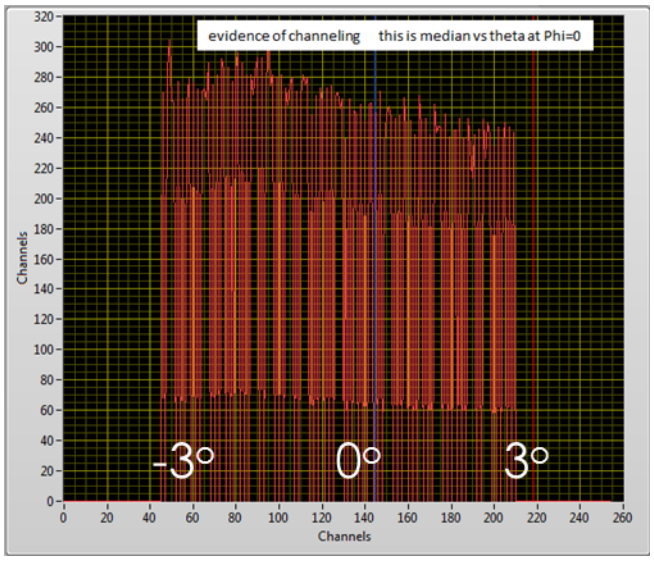

Figure 16: Median filtered IBIC pulse height distribution for 50 keV Li+ on the Amptek diode. The maximum at -1.5 degrees indicates that is the setting where ion channeling occurred.

We anticipated, based on the discussion and figure in Section 2.3.2, that the IBIC peak height would be a maximum when the Si diode crystal was set for an <001> axial channeling condition. This indeed was observed when θ=-1.5^o . The width of this channeling angle is ~2^o. This is in fair agreement with a channeling theory and program, also developed by this LDRD, of this channeling angular width of 2.59^o [16,17].

4.4 Problems with the nanoImplanter

Unfortunately, the nanoImplanter continued to have HV problems going above 50kV, and this precluded using a 100 keV Li+ beam. In fact the entire nI accelerator system went out of operation for the last two weeks of September when the IBIC scans of collision cascades was scheduled. The experiment will therefore have to be completed in FY17, and hopefully the QASPR program will support that. At that time the nI will be fixed and permit increasing the Li+ energy to 100 keV which will further improve the IBIC signal contrast and latteral beam resolution. With all these improvements that includes 1) more stable XY scan voltages, 2) higher Li energy, 3) the use of the Attocube for aligning the detector for ion channeling, 4) an improved LabView program for performing IBIC on the nanoImplanter, we fully expect to see incredible collision cascade structures caused by the Kr implants into the Amptek X-ray diode Si detectors.

5. CONCLUSIONS AND FUTURE WORK

Nanometer-sized clusters of atomic defects in semiconductors are known to be produced during collision cascades induced by high-energy neutrons. These clusters threaten the electrical operation of transistors, that are part of important circuits in weapons, but the basic physics underpinning of this degradation is uncertain. Vast quantities of such neutrons would be produced by the detonation of proximate nuclear weapons; therefore, this represents an important hostile radiation threat to weapon operation.

This LDRD has developed the hardware and software that will fill this understanding gap by performing an experiment that quantifies, coupled to a model that theoretically predicts, carrier recombination in the vicinity of a single cluster.

While we were quite disappointed that the poor operation of the nanoImplanter at the end of this project foiled our attempts to complete these experiments this FY, we are confident that with a future program like QASPR, these unique nano-Ion Beam Induced Current (IBIC) measurements will be accomplished. The underlying physics of electron-hole recombination in the proximity of collision cascades and defect clusters will then be revealed.

Again, all of the components required to perform this one-of-a-kind experiment were completed by this LDRD:

Summarizing the accomplishments of this LDRD:

1. The lightest ion possible - Li+ - was obtained on the nanoImplanter for the first time
2. It was discovered that a beam's intensity can be reduced to 100s of ions/sec while still maintaining a good focus
3. An ion channeling theory and program was developed, significantly improving the calculation of channeling half-angles for axes and planes up to (555).
4. The very first Ion Beam Induced Charge (IBIC) measurements were made where the beam channeled into the crystalline diodes.
    a. He, Li and Kr ions were used for this channeling
    b. Effects on the IBIC signal of ions scattering out of and into channels was observed for the first time
    c. Discovered that the IBIC signal resolution improved by channeling
    d. And beam spot resolution should be maintained due to the avoidance of scattering
5. The energy resolution of IBIC was improved from 13 keV to 0.15 keV
6. The reduction of the IBIC signal produced by Si and Li ions was observed for moderate fluences of Si.
7. Three IBIC theories were developed
    a. One calculated the Gunn potential responsible for IBIC
    b. Another calculated the IBIC signal expected to be observed around single defect clusters

c. The Marlowe binary collision code was used to predict the different levels of ionization of ion beams that channel and those that don't.
    i. It is this ionization that produces e-h's that produce the IBIC signal
    ii. For channeling, the Marlowe significantly over estimated this ionization, indicating that the ionization caused by primary collision recoils is not handled correctly in Marlowe.

8. The Li+ channeling-IBIC system is in complete operation on the nanoImplanter in the IBL, and ready to be used in future programs such as QASPR.

6. REFERENCES

1. Overview of QASPR (March 2011) SAND2011-1764P
2. Wampler, William R., and Samuel M. Myers. “Transport-reaction model for defect and carrier behavior within displacement cascades in gallium arsenide”, SAND Report SAND2014—1153, 2014
3. Wampler, William R., and Samuel M. Myers. "Model for transport and reaction of defects and carriers within displacement cascades in gallium arsenide." Journal of Applied Physics 117.4 (2015): 045707.
4. Auden, E. C., Doyle, B. L., Bielejec, E. S., Pacheco, J. L., Vizkelethy, G., & Abraham, J. B. S. (2015). “Charge Collection Imaging of Single Collision Cascades Using Nano IBIC” , Sandia Report No. SAND2015-4575C.
5. E. C. Auden, B. L. Doyle, E. Bielejec, G. Vizkelethy, and W. R. Wampler, "Optimization of a Low Noise Detection Circuit for Probing the Structure of Damage Cascades with IBIC," Physics Procedia, vol. 66, pp. 561-567, Jan. 2015.
6. E. C. Auden, J. L. Pacheco, E. Bielejec, G. Vizkelethy, J. B. S. Abraham, and B. L. Doyle, "Sub-Micron Resolution of Localized Ion beam Induced Charge Reduction in Silicon Detectors Damaged by Heavy Ions," Transactions on Nuclear Science, vol. 62, no. 6, pp 2919-2925, Dec. 2015.
7. http://www.linearsystems.com/assets/media/file/datasheets/DPAD.pdf
8. http://amptek.com/products/a250-charge-sensitive-preamplifier/
9. http://amptek.com/products/a250cf-coolfet-charge-sensitive-preamplifier/
10. http://amptek.com/products/xr-100cr-si-pin-x-ray-detector/
11. http://www.semefab.com/
12. E. C. Auden, J. L. Pacheco, E. Bielejec, G. Vizkelethy, J. B. S. Abraham, and B. L. Doyle, "Sub-Micron Resolution of Localized Ion beam Induced Charge Reduction in Silicon Detectors Damaged by Heavy Ions," Transactions on Nuclear Science, vol. 62, no. 6, pp 2919-2925, Dec. 2015.
13. http://www.attocube.com/attomotion/
14. https://www.fastcomtec.com/
15. Robinson, M "Computer simulation studies of high-energy collision cascades1". Nuclear Instruments and Methods in Physics Research Section B. 67: 396. (1992).
16. B.L. Doyle, “Parameterization of ion channeling half-angles and minimum yields”, Nuclear Instruments and Methods-B, Vol. 371 (2016) 63-68.
17. Barney L. Doyle, Aldo Corona, Anh Q. Nguyen, “Ion Channeling Revisited”, Sandia report SAND2014-18131, Sept. 2014.

DISTRIBUTION

1	MS0899	Technical Library	9536 (electronic copy)

For LDRD reports, add:

1	MS0359	D. Chavez, LDRD Office	1911

Sandia National Laboratories